Available online at www.sciencedirect.com
SCIENCE DIRECT®
Medical Image Analysis 9 (2005) 376–393
MEDICAL IMAGE ANALYSIS
www.elsevier.com/locate/media

Tagged magnetic resonance imaging of the heart: a survey

Leon Axel [a,b,*], Albert Montillo [b], Daniel Kim [a]

[a] Department of Radiology, New York University School of Medicine, 650 First Ave., Room 600A, New York, NY 10016, United States
[b] Department of Computer and Information Science, University of Pennsylvania, Levine Hall, 3330 Walnut Street, Philadelphia, PA 19104-6389, United States

Received 6 January 2004; received in revised form 28 December 2004; accepted 31 January 2005
Available online 4 May 2005

Abstract

Magnetic resonance imaging (MRI) of the heart with magnetization tagging provides a potentially useful new way to assess cardiac mechanical function, through revealing the local motion of otherwise indistinguishable portions of the heart wall. While still an evolving area, tagged cardiac MRI is already able to provide novel quantitative information on cardiac function. Exploiting this potential requires developing tailored methods for both imaging and image analysis. In this paper, we review some of the progress that has been made in developing such methods for tagged cardiac MRI, as well as some of the ways these methods have been applied to the study of cardiac function.

Keywords: Tagged MRI; Cardiac function; Image analysis; Magnetic resonance imaging; Heart

1. Introduction

Although heart disease is of great clinical importance, there are many limitations of the conventional methods used to assess cardiac function. Clinical assessment of a patient's symptoms and their functional or exercise tolerance impairment correlates poorly with conventional imaging-derived measurements of their cardiac function, such as ejection fraction (EF). Furthermore, although there is a good overall statistical correlation between measures such as EF and the subsequent clinical course, in any individual subject they are of poor predictive value. In addition to the limitations of conventional function measures for clinical assessment, they are also very limited as tools to investigate mechanical factors involved in normal and abnormal cardiac function or to aid in the design and evaluation of new therapies for impaired cardiac function.

A major source of the limitations of conventional cardiac function measurements is their inability to follow the motion of individual portions of the heart wall. The availability of tomographic imaging methods, such as conventional magnetic resonance imaging (MRI), has improved the reliability of global cardiac function measurements, such as the ventricular volumes or stroke volumes. However, the paucity of reliably identifiable landmarks in the heart wall largely limits the assessment of regional cardiac function to simply tracking the motion of the endocardial or epicardial boundaries of the heart wall in such images and trying to infer the corresponding distribution of intramural motion. Such contour tracking is subject to potential error due to the inability to reliably correct for the through-plane component of the 3D motion of the heart relative to the fixed image plane. Furthermore, any other components of the heart wall motion, such as torsional components between different "rings" of the heart muscle along the

* Corresponding author. Tel.: +1 212 263 6248; fax: +1 212 263 7541.
E-mail addresses: leon.axel@med.nyu.edu (L. Axel), montillo@seas.upenn.edu (A. Montillo), dan.kim@med.nyu.edu (D. Kim).

1361-8415/$ - see front matter © 2005 Elsevier B.V. All rights reserved.
doi:10.1016/j.media.2005.01.003

axis of the heart or within-wall components of motion such as shearing or transmural variation of radial thickening, are essentially invisible with conventional tomographic imaging methods. Although qualitative assessment of regional cardiac motion by visual evaluation of dynamic displays of tomographic MRI or ultrasound data can be clinically very useful, it is also very subjective and difficult to compare between different examinations and different subjects.

There is intrinsic sensitivity of MRI to motion, as was recognized even early in the experience with in vivo nuclear magnetic resonance, before the development of MRI per se. This motion sensitivity stems primarily from two sources: (1) There is persistence (within the limits of the relaxation times) of local alterations in the magnetization of material (such as the heart wall), even in the presence of motion; this allows us to deliberately (and non-invasively) produce local perturbations of the magnetization of the heart wall that will be visible in the images and will serve as material tags within the heart wall. (2) The motion of excited (signal-producing) nuclei in the presence of the magnetic field gradients used during MRI data acquisition has the potential to induce a phase shift of their signal due to the motion of the nuclei, e.g., due to heart wall motion, that is related to the velocity of or distance traveled by the nuclei. While these effects can be seen in the course of the performance of conventional MRI of the heart (Van Dijk, 1984), we can also design modified MRI pulse sequences to produce images that specifically exploit these effects, in order to use them to quantitatively assess motion. Although these MRI motion characterization methods have previously been primarily applied to the study of blood flow, they can also be used to study the motion of the heart wall (as discussed in Section 5). We will here focus on a review of some aspects of the use of magnetization tagging in MRI of the heart to evaluate regional cardiac function. This will include consideration of some aspects of the imaging process itself, some approaches to the process of analyzing the tagged images and extracting quantitative information about cardiac function from them, and some initial results of using these tagged MRI methods to study cardiac function in health and disease or models of disease. We will present a survey of some current approaches to tagged MRI, rather than original results, and will compare tagged MRI to some other conventional methods for cardiac motion assessment.

2. Tagged MRI methods for imaging local cardiac function

Myocardial tagging with tag analysis is an MRI technique that can be used for quantitative assessment of intramyocardial contractile function (Zerhouni et al., 1988; Axel and Dougherty, 1989a). The principle of myocardial tagging is based on producing a spatial pattern of saturated magnetization within the heart wall, e.g., at end diastole, and then imaging the resulting deformation of the pattern as the heart contracts through the cardiac cycle. Tagged MR imaging can be divided into two separate stages: (1) producing a spatially modulated pattern of saturated magnetization in the heart using a combination of RF and gradient pulses, and (2) imaging the deformation of the pattern using virtually any desired electrocardiogram (ECG)-gated pulse sequence. The following sections describe the two stages of tagged MRI in more detail.

2.1. Tagging methods

The concept of spin tagging was first used for measurement of blood velocity (Morse and Singer, 1970). Zerhouni et al. applied this concept for visual assessment of myocardial function using selective radio-frequency (RF) excitation to produce a few saturated parallel planes within the heart wall (Zerhouni et al., 1988). Axel and Dougherty subsequently developed a more efficient method, spatial modulation of magnetization (SPAMM), that uses non-selective excitation to produce saturated parallel planes throughout the entire imaging volume within a few milliseconds (Axel and Dougherty, 1989a). The saturated tags fade due to T1 relaxation and repeated RF excitations during imaging (Reeder and McVeigh, 1994). One approach to minimize the tag fading due to T1 relaxation is the use of complementary SPAMM (CSPAMM) (Fischer et al., 1993). This technique acquires two tagged images with SPAMM patterns that are 180° out of phase with each other and subtracts them. A disadvantage of CSPAMM is that it increases the image acquisition time. Other researchers have developed various tagging schemes, including higher-order SPAMM (Axel and Dougherty, 1989b), DANTE (Mosher and Smith, 1990), sinc-modulated DANTE (Wu et al., 2002), radial tags (Bolster et al., 1990), and hybrid SPAMM/DANTE (McVeigh and Atalar, 1992); each such tagging method has relative advantages and disadvantages (Table 1). The limiting factor in the fineness of the tagged pattern that can be imaged is the resolution of the imaging method, rather than the production of the tags themselves. The tag production method chosen can be used as a "conditioning" module, prior to imaging with essentially any desired cardiac MRI sequence. Fig. 1 shows an ECG-gated 1-1 SPAMM sequence that produces a sinusoidal variation of the magnetization along the direction of the gradient (typically chosen along the frequency-encoded direction in the image). In this example, a sinusoidal variation of the magnetization is encoded immediately after a trigger signal from the ECG. Subsequently, any desired imaging pulse sequence can be used to acquire

Table 1
Some tagging pulses

	Description	Advantages	Disadvantages
Selective tags	Selective saturation bands	Flexible	Inefficient
1-1 SPAMM	Gradient between RF pulses	Fast, efficient	Sinusoidal tags
CSPAMM	Difference of phase-shifted 1-1 SPAMMM	Longer net tag persistence; suppresses untagged blood	Longer image acquisition; sinusoidal tags
Higher order SPAMM	Longer pulse trains with different strengths	Sharper tags	Slightly longer to play out
DANTE	Train of RF pulses during gradient	Faster than pulsing gradient	Sinc-shaped tags if same RFs; requires hard RF
Sinc-DANTE	Sinc modulation of RF pulses	Sharper tags	Requires hard RF
SPAMM/DANTE	Reduced gradient during RF	Less demanding on RF than full DANTE and on gradients than fully pulsing them	Less benefits than either alone, too
Radial	Selective tags in radial pattern	Better orientation for assessing circumferentially	Inefficient to create

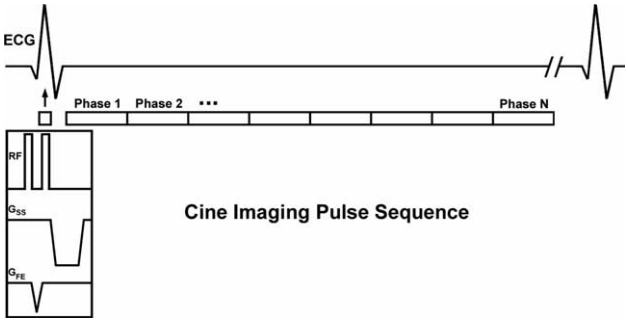

Fig. 1. An ECG-gated 1-1 SPAMM sequence comprised of two 90° RF pulses and a gradient pulse. The magnetization modulation gradient is typically applied along the frequency-encoding direction. A spoiling gradient is applied along the slice-select direction to dephase the residual transverse magnetization. Virtually any desirable pulse sequence can then be used to sample images over multiple cardiac phases. FE: frequency-encoding; SS: slice-select.

images over multiple cardiac phases. Fig. 2 shows representative tagged images of a mid-ventricular short-axis view at early systole and end systole. Cine images are typically acquired over multiple cardiac cycles within a breath-hold duration of 10–20 s. Myocardial tags fade as a function of T1, which is on the order of 850 ms. Therefore, myocardial tags are produced anew with each cardiac cycle in order to compensate for relaxation-induced fading. Multiple researchers have validated the reliability of tagged MRI as a reflection of the motion of the underlying tagged material with independent optical measurement in phantoms (Young et al., 1993; Moore et al., 1994) and with independent sonomicrometric measurement in vivo (Lima et al., 1993; Yeon et al., 2001). The aforementioned techniques have successfully been applied for the assessment of 2D intramyocardial function. However, these 2D techniques are prone to the effects of through-plane motion, as the images acquired at different cardiac phases may not represent the same slice of the myocardium. The slice-following method has been proposed to account for the effects of through-plane motion (Rogers et al., 1991; Fischer et al., 1994).

The heart is a 3D structure with a highly complex contraction pattern. Thus, it has been suggested that a 3D model of the cardiac motion and strain may be more

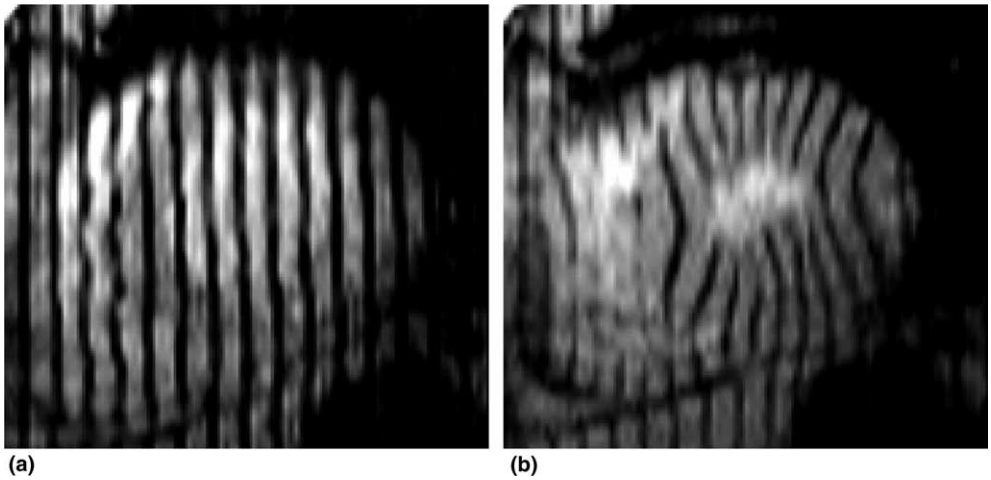

Fig. 2. Representative tagged images of a mid-ventricular short-axis view at early systole and end systole. These images were acquired using a 5-7-9-7-5 SPAMM module and an optimized FGRE-EPI sequence (available as movie file, see Appendix A).

suitable to compare, for example, with the 3D fiber architecture of the heart wall. There are two possible approaches for the reconstruction of a 3D model of cardiac motion and strain. The first approach is to combine multiple 2D short-axis and long-axis views (Young and Axel, 1992; Moore et al., 2000). The second approach is to perform 3D tagged imaging (Ryf et al., 2002). We will discuss their relative merits in the following section.

2.2. Imaging methods for tagging

Recent developments in commercial gradient systems have provided an enormous increase in imaging speed. Currently, various breath-hold sequences are available for 2D myocardial tagging, including: segmented *k*-space gradient echo (McVeigh and Atalar, 1992), interleaved gradient-echo-planar imaging (Tang et al., 1995; Stuber et al., 1999a,b,c), hybrid gradient-echo/echo-planar imaging (Reeder et al., 1999; Kim et al., 2003; Epstein et al., 1999), interleaved spiral imaging (Ryf et al., 2004), undersampled projection reconstruction (Peters et al., 2001), and balanced steady state free precession (Herzka et al., 2003; Zwanenburg et al., 2003). Each pulse sequence entails a tradeoff between imaging speed and artifacts or signal-to-noise ratio (SNR) (Table 2). Therefore, imaging considerations must be taken into account when choosing and designing the appropriate tagging protocol, such as tag contrast (defined as the contrast-to-noise ratio between the tagged and non-tagged myocardium), and spatial and temporal resolution.

Some basic guidelines for myocardial tagged MRI have become apparent: (1) The spatial resolution of the strain computed from the tagged images is nominally defined as the distance between two adjacent tags. Therefore, the spatial resolution of the imaging sequence must be able to provide at least two tags across the myocardial wall to assess radial strain. (2) The temporal resolution must be high enough to avoid motion blurring of tags. This condition is particularly important for tagging studies on diastolic dysfunction (e.g., the rapid filling phase of diastole) and wall motion abnormalities induced by pharmacologic stressors such as dobutamine, which also increases the heart rate. (3) Pulse sequences with a high data acquisition efficiency (e.g., spiral and EPI sample a large trajectory of *k*-space per RF excitation) produce higher tag contrast and longer tag persistence than conventional gradient echo sequences, but they are also more prone to sources of image artifacts such as static magnetic field inhomogeneity and motion.

Typical breath-hold techniques pose challenges for achieving all three imaging considerations within a clinically acceptable breath-hold duration of 15–20 s. One approach to reduce the scan time (breath-hold duration) is acquiring two orthogonal line-tagged images with asymmetric *k*-space sampling, rather than a grid-tagged image with isotropic resolution. In Fig. 3, a line-tagged image and its corresponding *k*-space image are shown in order to illustrate this point. In this example, a set of parallel lines is saturated perpendicular to the frequency-encoding axis (nominally x). The Fourier components of this tagged image are located in *k*-space near $k_y = 0$ (Fig. 3(b)), and they shift and rotate in *k*-space as the tags deform through the cardiac cycle. As a result, approximately 30–40% of the *k*-space may be sufficient to sample the Fourier components of a line tagging pattern (McVeigh and Atalar, 1992; Fischer et al., 1993). An orthogonal tagged image can be acquired by swapping the frequency- and phase-encoding axes. The combined images provide equivalent isotropic resolution in the directions most important for resolving the tags.

Here we discuss the relative advantages and disadvantages of 2D and 3D tagging. Contiguous multi-slice imaging and full 3D imaging have equivalent data acquisition efficiency. A major distinction between the two methods is that multi-slice acquisition depends on proper selective excitation while 3D imaging depends on proper gradient modulation. A major advantage of contiguous multi-slice imaging is that it is straightforward to implement. Disadvantages of multi-slice imaging are that it typically produces imperfect slice profiles and may not be able to achieve contiguous thin slices. Volumetric imaging can potentially overcome these limitations and provide an additional benefit of higher signal-to-noise ratio (SNR). However, 3D imaging also requires a form of respiratory tracking, which may be more difficult to implement. In both cases, the

Table 2
Some pulse sequences for imaging tagging

Method	Advantages	DIsadvantages
Segmented gradient echo	Standard imaging	Less time-efficient
Echo-train readout (EPI)	More time-efficient; less tag fading with fewer RFs	More vulnerable to poor shimming
Spiral	Oversampling the center of *k*-space may improve blood-myocardium contrast	Inefficient sampling of *k*-space, as tagged peaks are located away from the center; as for EPI readout
Projection-reconstruction	As for spiral	As for spiral
SSFP	Higher SNR	More vulnerable to poor shimming; transient artifacts from tagging
3D imaging	Better spatial registration	Cannot breath-hold; oblique imaging of walls

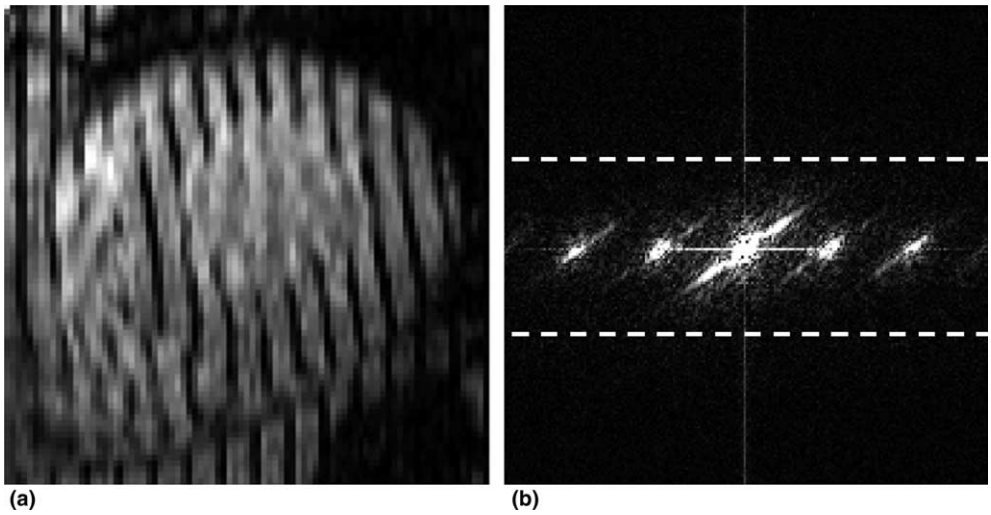

Fig. 3. A line-tagged image (a) and its corresponding k-space image (b). The Fourier components of this tagged image are located in k-space near $k_y = 0$, and they shift and rotate in k-space as the tags deform through the cardiac cycle. As a result, approximately 30–40% of the k-space is sufficient to sample the Fourier components of a line-tagging pattern. The area covered by the dotted lines represents the region of k-space most important for resolving the tags.

subject needs to maintain a consistent respiratory pattern and body position for the duration of the imaging, in order to able to achieve consistent 3D reconstruction of the motion.

Respiratory motion artifacts are typically suppressed by breath holding (Edelman et al., 1991) or navigator-based gating to the respiratory cycle (Korin et al., 1990; Ehman and Felmlee, 1989). Although the breath-hold technique is the simplest method for suppressing respiratory artifacts, it also poses challenges for achieving adequate SNR within a clinically acceptable breath-hold duration of 15–20 s and for spatially registering multiple 2D images acquired with sequential breath holding that may not be completely consistent. Navigator methods can be used to track the diaphragm motion and reduce motion artifacts by post-processing (Sachs et al., 1995). The main disadvantage of using navigators for cine tagging is that they take up a portion of the imaging duty cycle and thus limit time available for image acquisition. Alternatively, combined ECG triggering and respiratory gating may be used to reduce motion artifacts in cardiac MRI (Ehman et al., 1984; Yuan et al., 2000). This alternative method is relatively straightforward to implement and requires less patient cooperation, but it can also increase the scan time by as much as navigator methods (typically by 2–4 times).

Myocardial tagged MRI is a promising technique for quantitative assessment of intramyocardial function. An integrated approach that combines fast imaging pulse sequences, joint ECG and respiratory gating, parallel imaging, and dedicated cardiac coils may allow 3D tagging to be more practical. Future developments and refinements in 3D tagging may lead to more accurate 3D models of cardiac motion and strain.

3. Tagged image analysis

The analysis of tagged cardiac cine MR images yields measures of global and regional cardiac function. The analysis of tagged MR images may involve several steps, including: (1) image preparation, (2) boundary surface extraction, (3) tag tracking, (4) 3D motion reconstruction, and (5) intra/intersubject comparison, statistical model formation and computer-aided diagnosis.

Image preparation facilitates subsequent analysis through steps such as: (1) removing image artifacts such as RF inhomogeneity, (2) suppressing noise and (3) standardizing the intensities across subjects. Global function measures of the heart, such as ventricular mass, stroke volume, ejection fraction, and cardiac output (given the heart rate), can be computed from tagged cardiac MR images through the extraction of the boundary surfaces of the right ventricle (RV) and left ventricle (LV). These measures are comparable to those from non-tagged images (Dornier et al., 2002). These boundary surfaces can also be used to determine useful local functional measures, such as wall surface curvature (Moses and Axel, 2004) and wall thickening, and to facilitate tag line tracking and 3D motion reconstruction (Haber et al., 2000b; Park et al., 2003). By tracking the motion of the tag lines within images of the heart wall (Qian et al., 2003; Guttman et al., 1994; Amini et al., 1994; Osman et al., 1999), deformation fields can be computed. Given a two-dimensional array of tag motion data, a 2D deformation field can be calculated. Combining the motion from orthogonal tag and image plane orientations, a full 3D deformation field and related strain maps can be reconstructed, which more fully characterize the motion of the myocardium (Haber et al.,

2000b; Park et al., 1996, 2003; Declerck et al., 1998). When both the boundaries and the tag lines are extracted, information such as stress tensor maps can be derived (Hu et al., 2003a,b), and intra/intersubject comparisons can be made with statistical models of regional contractility (Augenstein and Young, 2001), enabling computer-aided diagnoses. In addition, given the boundary and regional contractility data, the contractility data can be spatially fused with data from other modalities, including perfusion MR, electrical activation (Sermesant et al., 2002) or blood flow (McQueen and Peskin, 2000), thus forming a more comprehensive evaluation of the heart.

Manual and even semi-automated image analysis methods, such as user-guided active contours or "snakes" (Fig. 4) (Kraitchman et al., 1995), for boundary and/or tag segmentation are too time consuming for routine clinical application, generally requiring many hours per subject. To make tagged MR clinically viable, an automated analysis method is essential (Amini and Prince, 2001). Moreover, the trend in imaging is towards increased spatiotemporal resolution, which further increases the need for highly automated analysis methods. Although there are many challenges in developing such an automated system, it is an active area of research.

3.1. Image preparation

Image preparation typically involves three principal steps: (1) suppression of background intensity variation due to non-uniform RF fields, (2) suppression of thermal noise, and (3) normalization of image intensities, which intrinsically vary in MRI from subject to subject or even for the same subject upon repeated scans. Several researchers have developed general methods for suppressing background intensity variation in MR images (Sled et al., 1998; Wells et al., 1996), while others have developed methods which are more specifically tailored to tagged MR (Montillo et al., 2003a; Axel et al., 1987). Suppression of thermal noise in MR images has received much attention. Some methods target noise suppression in isolation (Saha and Udupa, 2001), while others combine the suppression of background intensity variation with noise suppression (Montillo et al., 2003b). The lack of an absolute scale for MR image intensities, which can cause the same tissue to vary in nominal intensity from one subject to the next, necessitates an intensity normalization method. While this problem has received less attention, a histogram modification method previously proposed and tested on brain MRI (Nyul et al., 2000) has recently been successfully adapted for tagged cardiac MRI (Montillo et al., 2003a). When the normalization is applied to successive frames from the same subject, the method has also been shown to help suppress the effects of tag fading.

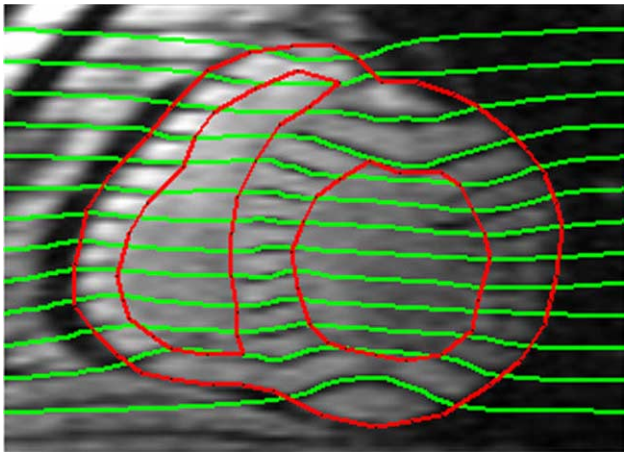

Fig. 4. Analyzed short-axis tagged image. In red are manually drawn contours of endo- and epicardial surfaces. In green are the tag lines tracked using active contours. These active contours rely on external forces derived from the image, as defined by the endo- and epicardial surfaces and the dark tag lines, to minimize their energy function. The tag active contours only respond to image forces within the heart wall.

3.2. Boundary surface extraction

The extraction of the endocardial and epicardial surfaces of the heart from tagged MR images is challenging for several reasons including: (1) image artifacts and noise should be suppressed and the tag lines should be removed to help avoid interference with boundary detection, (2) features outlining the boundaries must be identified, (3) the image data generally samples the volume of the heart with gaps and nonuniform spacing between image planes, and the geometry of the heart is complex, making initialization of boundary surfaces difficult.

As a result, most researchers have resorted to manual entry for this task and focused on development of methods for other aspects of image analysis (Young, 1999; Haber, 2000a; Park et al., 1996, 2003; Declerck et al., 1998; Ozturk and McVeigh, 1999) that require the boundary surfaces as input. Earlier technique development focused on semi-automated methods in which user-guided active geometry (Kraitchman et al., 1995; Young et al., 1995; Kumar and Goldgof, 1994) was employed to locate the boundaries of the myocardium. Other methods, which are either largely or completely automated, rely upon morphological or matched-filter operations to enable edge detection. Guttman et al. (1994) proposed a method to locate the LV contours using a sequence of steps including: (1) manual initialization of a ROI containing the heart, (2) application of several morphological operations and (3) the minimization of a cost function using dynamic programming; this method was extended to 3D (Goutsias and Batman, 2000). Guttman et al. (1997) located the LV contours through a series of morphological operations followed by a marker-driven watershed segmentation. Several researchers (Denney, 1997; Chen and Amini, 2001) have

applied Markov random fields to partially segment the myocardium; however, they have stopped short of actually segmenting the contours themselves. Montillo and Metaxas (2000) developed a fully automated method that computes the location of the heart and segments the epicardial and endocardial surfaces for a biventricular model, including the bifurcation of the RV into inflow and outflow tracts and the exclusion of fat from myocardium. This method combines grayscale morphology and 2D active geometry and integrates the image preparation step into the overall data analysis. Recently, this method was extended to fit 3D surfaces, using both short- and long-axis image sets (Fig. 5) (Montillo et al., 2003c). This extension included the development of a method for extracting 3D image forces from the relatively sparse set of parallel and radially arranged 2D images (Fig. 6) and applying them to deform a single active epicardial surface model (Fig. 7), as well as endocardial models of the RV and LV (Fig. 8).

3.3. Tag tracking

Currently, most tagged MRI data consists of two or three sets of 2D images acquired from parallel planes through the thoracic region or from planes arranged in a radially sampled pattern and intersecting at roughly the long axis through the LV. During acquisition of this data, the tagging planes are created in the heart in three (mutually orthogonal) directions and these tag planes are then manifested as dark lines through the myocardium in the MR images. To reconstruct the myocardial motion, the intensity heterogeneity representing the tagged planes must be tracked over time. Since the tracking is constrained to the image plane, only limited components of the 3D myocardial motion can be recovered from a given set of 2D image data. Methods which have been proposed for extraction of motion data from tagged images have relied on using different aspects of the myocardial intensity heterogeneity, including: (1) tracking the dark tag lines as intensity minima, (2) employing optical flow or (3) using harmonic phase (HARP) methods. The latter two methods do not explicitly track the tags per se.

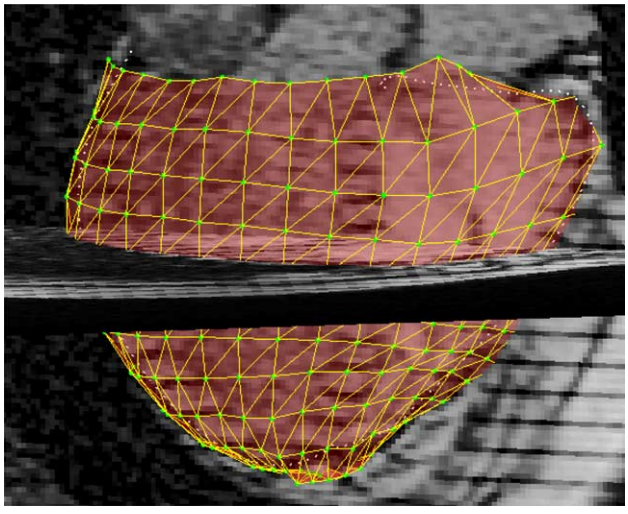

Fig. 5. Deformable 3D model of epicardium (colored shell), simultaneously fit to long- and short-axis tagged images (selected images shown). Dotted line shows manually drawn segmentation on the long-axis image.

The first method involves developing a model of the time-varying intensity profile of a tag line. The method typically begins by having a user manually identify the location of the tags in each imaged slice location at end diastole. Then the method may use an intensity model as a template to search the image to find, for each tag line, the next most probable location of the tag. Alternatively, the tags themselves can be segmented using approaches such as morphological operations to locate dark lines in the image (Guttman et al., 1994), matched filters (Chen and Amini, 2001; Young, 1998) or a Gabor filter bank (Qian et al., 2003). While the latter two techniques tend to be relatively robust with respect to tag fading, a limitation of all tag line tracking methods is that temporal correspondences are available only for pixels along the tag lines and not for the pixels in between them.

Optical flow-based techniques seek to overcome this limitation of the relatively sparse tag data and provide a spatially dense estimate of the 2D apparent motion field. The basis for this technique is the brightness constraint equation. This method involves estimating the spatial gradient of the intensity image, using finite differences of the intensities at neighboring pixels, as well as a temporal intensity derivative which is estimated by subtracting the intensity at a pixel from one time-frame to the next in a cine acquisition. While in some research (Denney and Prince, 1994) the time derivative of the brightness of a myocardial pixel is assumed to be zero, the brightness of a myocardial pixel may actually experience significant changes due to tag fading and through-plane motion. Therefore, several researchers have proposed strategies to either preprocess the images to suppress the effects of tag fading (Dougherty et al., 1999) or to model the tag fading portion of the variation based on the MRI physics (Prince and McVeigh, 1992). A somewhat related tag tracking approach is to use non-rigid registration to match corresponding tagged regions (Chandrashekara et al., 2002).

In 1-1 SPAMM tagging pulse sequences, tags are created with a sinusoidal cross-sectional intensity profile. At any point on or between the tags, the tissue has both a magnetization intensity and a spatial phase of the periodic tag magnetization pattern, which are dependent on position. Researchers have shown that the phase of the tag modulation pattern can be extracted from the image and this phase can be used to label the pixels in the myocardium. The HARP technique uses such an approach

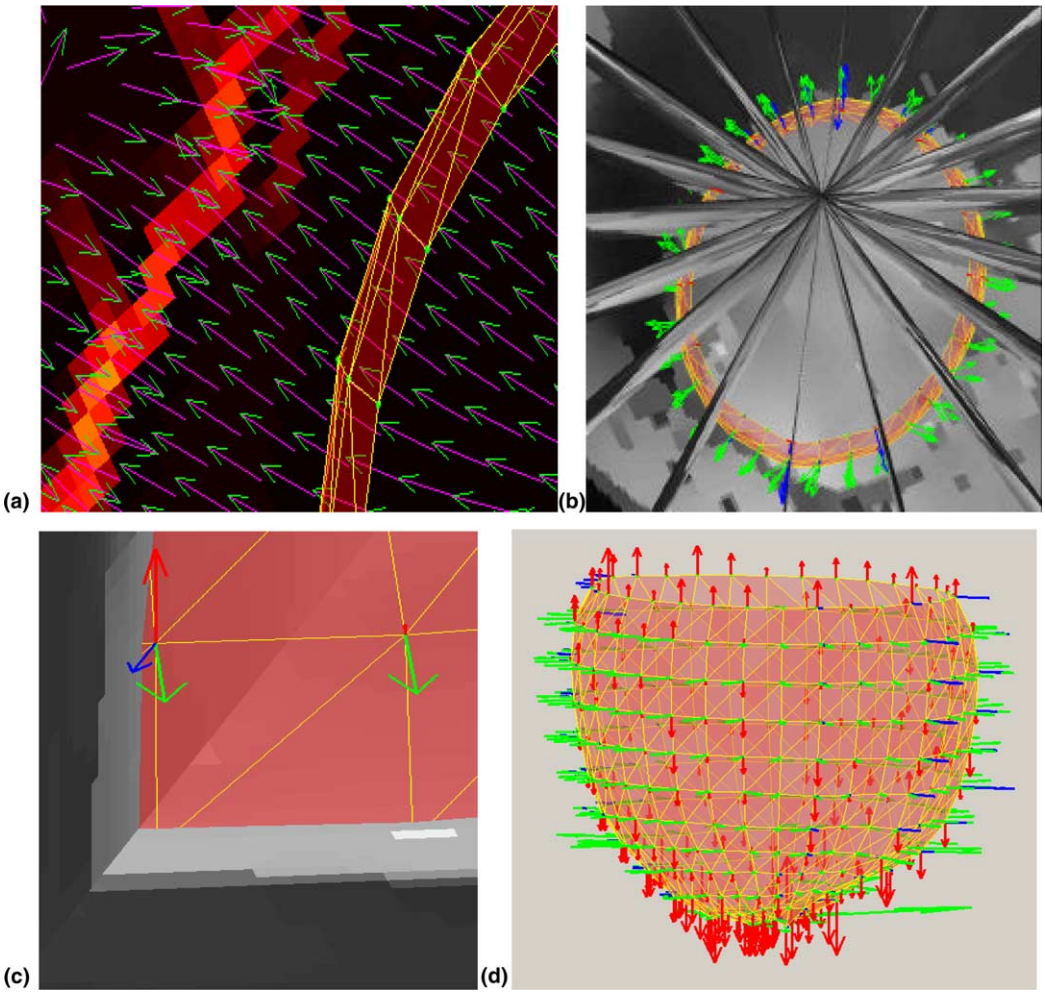

Fig. 6. Gradient vector flow forces are derived from an edge map from each preprocessed 2D image and act as external forces that fit the model to the patient data. (a) Forces acting on model points in the image plane; axial image with model viewed from the head looking towards the feet. (b) Additional forces from the long-axis images also help fit the model. Forces from all data: both short- and long-axis image sets are combined and then extrapolated to the FEM model nodes neighboring each model/image plane intersection point. (c) Forces from selected images acting on a node. (d) Forces acting on all model nodes from all image data.

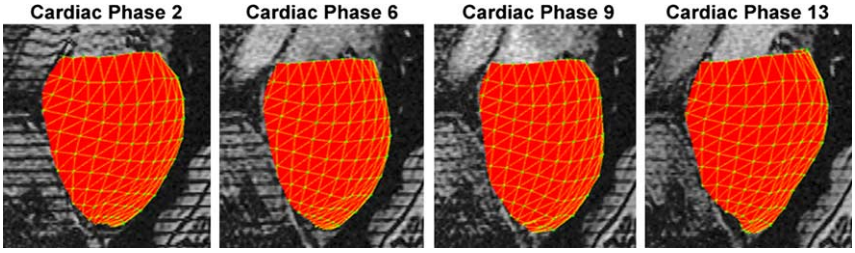

Fig. 7. Superimposing the 3D epicardial surface model over long axis images shows the shape of the contraction over systole and relaxation in diastole. The model contracts throughout systole (phases 2–9) and expands during diastole (phases 9–13).

to track the phase of the tissue tagging pattern in "angle" images (Osman et al., 1999; Garot et al., 2000). The angle images are derived from the phase of the complex image which is computed from the Fourier transform of the immediate neighborhood of the first harmonic peak (corresponding to the frequency of the sinusoidal tags) in the spectral domain data. This can be acquired either directly from the MRI system or from an inverse Fourier transform of the tagged image. One can view this method as effectively optical flow in the spectral domain, in which the constant pixel brightness assumption is replaced by the potentially more reliable constant pixel phase assumption. As the angle image reflects the effective phase of the tag pattern in the neighborhood of a point, it may not be reliable near the edges of the heart wall due to partial volume effects, as

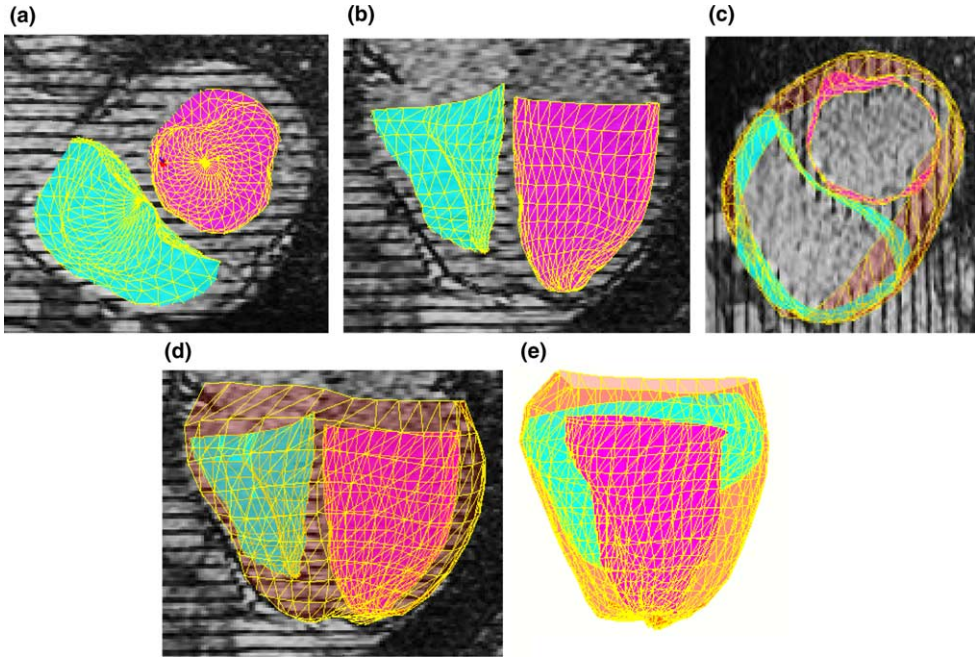

Fig. 8. Fitted endocardial surface models of the LV and RV from various views: (a) axial and (b) coronal. Including fitted epicardial surface model: (c) axial, (d) coronal, (e) sagittal.

discussed further below. Typically, the baseline phase is subtracted from the subsequent angle images to track the motion of the tag pattern. Note that the aliasing of the phase for shifts greater than 360° can lead to ambiguity equivalent to the "off-by-one" (or more) problem in tracking tags explicitly. If low spatial resolution is adequate, then just the spectral domain data near the first harmonic can be sampled by the MRI scanner (which intrinsically acquires images in the spectral domain), in order to increase the speed of acquisition of angle images used to track the phase of the tag pattern within the myocardial tissue.

All of the above methods are ill posed: thermal noise and image artifacts can cause ambiguities in the tracking of tag, optical flow or phase features. As a result, researchers have used regularization methods to find a motion field which balances fidelity to tag features with a smoothness constraint imposed on the overall motion field. While these methods often rely upon empirically chosen coefficients to adjust the tradeoff between these constraints, the regularization is often well worth the added effort. A variety of active geometry methods have been used to regularize intensity-based tag line tracking, including interlocking grids of 1D splines (Kraitchman et al., 1995), deformable templates and thin plate splines (Amini et al., 1998) and 2D B-splines (Amini et al., 1998). Temporal regularization approaches have also been used (Clarysse et al., 2000). Optical flow techniques have been cast in a variational framework (Prince and McVeigh, 1992). Harmonic phase approaches have also been regularized, using B-splines and finite element models (Deng and Denney, 2003; Haber et al., 2001).

All of the above tracking methods tend to be problematic near the boundary, where the epicardial and endocardial surfaces often appear as dark lines and thus can be confused as tag features. The myocardium near the boundary is also particularly difficult to characterize because tag lines can appear or disappear due to a combination of: (1) through-plane motion of the myocardium and (2) the convexity of the myocardium. These conditions near the boundaries can cause failures for all the algorithms in several ways: (1) The intensity template used by the tag line tracking may lock onto the boundary instead of a tag. (2) The boundaries can occlude tags and can act as spurious matches which confound the optical flow solution. (3) The boundaries can introduce apparent shifts of the tagging pattern in subendocardial and subepicardial tissue, which can cause inaccuracies in the motion recovered from harmonic phase method. These methods may benefit by constraining the solution with the location of the boundaries, which can be extracted either manually (Young, 1999) or using an automated technique (Montillo et al., 2002, 2003c).

3.4. 3D Motion reconstruction

Once the tags and contours have been segmented and tracked on the set of 2D images, the 2D motion information can be compiled to reconstruct a description of the 3D motion. We will consider some aspects of this 3D reconstruction here.

When tracking the motion of a tag line in the image, only one component of the underlying motion can be

derived from the data (perpendicular to the original orientation of the tag line), while at tag line intersections, two components of motion can be measured. The tag lines from adjacent images can be stacked to form a tag sheet by inferring the correspondences either as: (1) an additional step from their position relative to the boundary contours (Park et al., 1996, 2003) or as (2) an inherent part of the process of tracking the tags (Kerwin and Prince, 1998). At tag sheet intersections, all three components of the motion can be measured (Kerwin and Prince, 1998; Amini and Prince, 2001). When using optical flow methods (spatial or spectral), two components of motion are typically available at every pixel. In general, it is not possible to measure three components of motion for any given point from 2D tagging methods; however, methods such as slice following (Fischer et al., 1994) or the SENC method (Osman et al., 2002) may help eliminate this limitation. Although 3D tagging approaches to 2D tagged MR imaging have been proposed, they are difficult to analyze.

A variety of methods have been proposed which can compile the 2D information into a dense, smoothly varying, 3D motion field. These methods (Young, 1999; O'Dell et al., 1995; Deng and Denney, 2003; Ozturk and McVeigh, 1999; Declerck et al., 1998; Huang et al., 1999; Park et al., 1996, 2003; Haber, 2000a; Radeva et al., 1997; Chen and Amini, 2001) typically involve fitting a model, using an optimization function which balances fidelity of the final 3D motion field to the 2D motion measurements and a smoothness constraint which either (1) interpolates missing information, such as motion between the sparse tag sheet intersections or (2) suppresses errors in optical flow or harmonic phase motion fields.

Several researchers (Park et al., 1996; Declerck et al., 1998; Ozturk and McVeigh, 1999) have modeled the motion of the LV with a reduced number of parameters in the hopes of obtaining a more revealing description of normal and pathological motion. Park et al. (1996) used spatially varying parameter functions to adapt a superquadric model to fit boundary contour and tag line motion information. Declerck et al. (1998) employed a 3D B-spline tensor product to reconstruct the inverse deformation field, and a 4D planispheric transform was then estimated from the backward transformations and semi-automatically segmented tag lines. The motion was modeled as a 4D continuous displacement function in time and space, and strain was derived by taking first order derivatives. More general splines, with somewhat higher number of parameters, have also been proposed, including both 3D splines (Radeva et al., 1997; Young, 1999; Chen and Amini, 2001), and 4D spline models (Huang et al., 1999) that include time as the fourth dimension.

These models often have difficulties capturing the motion of the apex. To compensate for this limitation, both prolate spheroidal coordinates (Young, 1998; O'Dell et al., 1995) and 4D planispheric coordinates (Declerck et al., 1998) have been used to increase the numerical stability over spherical coordinates when reconstructing the motion at the apex of the LV.

Recently, biventricular motion reconstruction methods have been developed. When the RV is included in the model, a single spheroidal coordinate system no longer suffices. One approach is to model the biventricular system as a patient-specific volumetric finite element mesh (Haber, 2000a). Another approach that has been used is to establish a common mesh for all subjects (Park et al., 2003). In the latter method, three superquadric surface models are fitted to the contour data of the RV and LV at the beginning of systole and then used to construct a generic mesh fit to these surface models. Park et al. (2003) also modeled the base of the RV, including the inflow and outflow tracts. The task of obtaining tag data in these narrow extensions of the RV, which undergo significant through-plane motion, is particularly challenging.

Several general trends are noted when the literature in tagged image analysis is examined. First, all of the steps required for the analysis of cardiac tagged images are active research areas, and the methods involved in each step are steadily improving. Second, there are at least two categories of methods. One category of methods aims at obtaining only the deformation field, without any attempt to locate the heart or the endocardial and epicardial surfaces and feature points. In the short term, this method appears most promising for real time strain computation. The other category of methods, potentially requiring somewhat more time, additionally aims at extracting the bounding surfaces of the heart ventricles and can be used for a wider set of applications. These methods have begun to be used to facilitate: (1) intrasubject comparison, (2) the construction of statistical models of cardiac physiology and pathophysiology (Augenstein and Young, 2001), (3) the formation of additional means of quantifying and visualizing that physiology (Hu et al., 2003a,b), (4) the determination of classical measures of cardiac function without requiring an additional imaging step (Dornier et al., 2002) and (5) fusing cardiac tagged MR with other sources of functional information (Behloul et al., 2001). Thirdly, there is a general trend towards modeling a greater extent of the heart. In the initial years after the introduction of tagged MR, only the left ventricle was studied; since then, cardiac models have grown to include the right ventricle and recently its inflow and outflow tracts. This trend is likely to continue into the atria and to include a more physiologically based model of the myocardium, complete with anisotropic fiber orientations and laminar sheets. We expect this will make the analyses more useful for the non-invasive characterization of the whole heart, both for clinicians as a viable diagnostic and

treatment monitoring tool and for researchers as a powerful investigative tool.

4. Applications of tagged cardiac MRI

While the methods of performing and analyzing tagged cardiac MRI described above are still under development, some interesting initial results of their use are already available. We will briefly review some representative examples below.

An important initial application of tagged cardiac MRI is the mapping of the normal patterns of heart wall motion. Previous imaging methods used to study heart wall motion have been limited largely to following the motion of the surface of the heart wall, due to the inability to track the position of specific material points in the images over time, while directly labeling material points within the wall with conventional invasive techniques, such as the implantation of metal beads or ultrasound crystals, are both invasive (and potentially alter the motion itself) and are limited to a relatively small number of such points that can be tracked in any individual subject. Thus, the more extensively sampled and non-invasively derived motion data available on the normal heart through tagged MRI studies can be used both to provide new insight into the normal function of the heart and to serve as a baseline against which to compare the findings in patient studies. In carrying out this normal motion analysis, we can look either at the 2D cardiac motion revealed in individual 2D tagged image sets obtained at given locations within the heart, or at the full 3D cardiac motion as reconstructed from "stacked" 2D image sets covering the heart or from image data acquired primarily as 3D image sets. In general, multiple sets of such tagged image data, acquired in multiple image plane orientations and with different tag orientations, will be needed in order to fully sample the motion, as described in the previous section. While a full 3D reconstruction of the motion would be preferable if there were no other constraints, the limited time generally available for imaging and image analysis may also make it valuable to examine 2D motion data as well, for example, in circumstances where the motion data is only a portion of the information to be obtained in an MRI examination.

The normal motion of the heart wall, as revealed by tagged MRI, is considerably more complex than the simple radial contraction and expansion one might naively assume from the simplified accounts in many textbooks (Zerhouni et al., 1988; Axel et al., 1992; Young and Axel, 1992; Young et al., 1994a,b; O'Dell and McCulloch, 2000; Moore et al., 2000; Bogaert and Rademakers, 2001; Clarysse et al., 2000). In addition to the radial motion, there is a significant rotational component to the motion, including a normal torsional motion around the ventricular long axis, such that the base and apex of the ventricle rotate in opposite directions during the cardiac cycle. Furthermore, there is a significant longitudinal component of the motion, with an axial gradient such that the apex of the ventricles moves relatively little while there is a relatively large excursion of the base of the ventricles, with a reciprocating motion of the atrioventricular valve plane such that it moves roughly along the long axis during the cardiac cycle. There are also other consistent normal regional variations in the motion, such as a greater excursion of the free wall of the ventricles than the septum, as well as consistent transmural differences in strain and shearing motions within the wall (relative to the conventional cardiac-based radial, circumferential and longitudinal directions). These gradients of the bulk motion of the heart wall are less apparent in the normal heart when we consider the distribution of the regional strain; this reflects the fact that the strain provides a more coordinate system-independent reference frame within which to analyze the regional motion. The normal effects of age on heart wall motion can also be studied with tagged MRI (Fogel et al., 2000; Fonseca et al., 2003). Although the LV is easier to study with tagged MRI than the RV, due to its normally greater wall thickness, we can use tagged MRI to study the motion of the normal RV as well (Fayad et al., 1998; Young et al., 1996; Haber, 2000a).

Torsion of the heart is an aspect of cardiac motion that was previously known through more invasive methods, but which is much more readily studied with tagged MRI (Lorenz et al., 2000). Tagged MRI reveals that the torsional and overall contraction phases of systole are somewhat out of phase, with the torsion predominantly occurring early in systole. Similarly, the untwisting portion of diastolic relaxation primarily occurs early in diastole. It has been proposed that the untwisting early in diastole may provide a measure of relaxation that is relatively independent of the filling volume of the heart ("preload") (Dong et al., 1999, 2001); the early twisting component of systole may be similarly relatively independent of the resistance to outflow ("afterload").

Hypertrophy in response to pressure overload (e.g., due to either poorly controlled arterial hypertension or aortic stenosis in the left ventricle or to pulmonary hypertension or pulmonary valvular disease in the RV) can ultimately lead to ventricular failure or sudden death (presumably due to arrhythmia related to changes in conduction of the wave of electrical activation through the altered muscle). The effects of pressure overload hypertrophy may be more sensitively demonstrated with tagging than with conventional global measures of cardiac function (Palmon et al., 1994; Stuber et al., 1999a,b,c; Sandstede et al., 2002). Although one ventricle may be primarily involved by hypertrophy, the other can be secondarily involved as well, either through the

effects of having their circulations in series or, more directly, through sharing a common wall, the interventricular septum (Dong et al., 1995). The motion of the hypertrophied RV itself appears to be altered from its normal patterns as well (Haber, 2000a). Hypertrophic cardiomyopathy (HCM) is an uncommon condition leading to focal or more diffuse thickening of the myocardium in the absence of pressure overload, with the affected areas having variable amounts of disorder in the muscle fibers and infiltration with fibrosis. The result is decreased contraction in the affected regions of the heart wall, which can be demonstrated with tagged MRI (Kramer et al., 1994; Young et al., 1994a,b).

Demonstration of motion alterations due to the common clinical condition of ischemia, decreased blood supply to the tissue (e.g., during stress studies), is a natural potential application of tagged MRI methods. Decreased or absent myocardial contraction is one of the earliest manifestations of ischemia, and is of obvious functional importance. Myocardial tagging with strain analysis has been shown to be more sensitive to regional wall motion abnormalities than quantitative wall thickening analysis (Goette et al., 2001), and dobutamine stress MRI combined with tagging (Scott et al., 1999) has been shown to be more sensitive to wall motion abnormalities than cine MRI (Kuijpers et al., 2003; Kraitchman et al., 2003). The subendocardial portion of the heart wall is the most vulnerable to the effects of ischemia, and the ability of tagged MRI to resolve transmural differences in function should make it more sensitive to the presence of such abnormalities than conventional imaging methods. The mechanical effects and evolution over time of myocardial infarction (irreversible tissue damage due to prolonged ischemia) are another promising area for study with tagged MRI. The infarcted region itself permanently loses the ability to contract, and this is manifested in the altered motion seen in tagged MRI. Tagging studies may help detect viability after infarction (Geskin et al., 1998; Croisille et al., 1999), although delayed enhancement studies may be simpler to use for routine applications. As mentioned above, tethering effects may cause an alteration of the motion of the adjacent regions and a discrepancy between the apparent area of motion abnormality and the actual area of infarction. Longitudinal studies of infarct evolution in patients or experimental models with tagged MRI (Kramer et al., 1996a,b; Marcus et al., 1997; Bogaert et al., 1999) may help elucidate the mechanisms of the clinical outcomes and could potentially help lead to better treatment methods.

Masses of the heart wall can produce local alterations of motion by replacing and locally "tethering" the myocardium. These local alterations of motion can be revealed with tagged MRI (Bouton et al., 1991). While the presence of a mass can often be seen more directly by its resulting local alteration of the contour or the intensity of the heart wall, tagged MRI can be very helpful in distinguishing between a local mass-like area of focal hypertrophic cardiomyopathy and a true mass (Bergey and Axel, 2000).

Constriction of the heart by pericardial disease can have visible effects on the cardiac motion in tagged MRI (Kojima et al., 1999). A common clinical question is whether a clinically observed impairment of cardiac function is due to interference with cardiac function, particularly diastolic filling, by the constrictive effects of pericardial disease ("constriction") or whether it is primarily due to restrictive primary disease of the myocardium itself ("restriction"). Conventional imaging criteria for distinguishing these conditions, such as the thickness of the pericardium, are not fully reliable. Tagged MRI may be able to help in distinguishing these conditions.

Conventional cardiac MRI is already playing an important role in the evaluation of congenital heart disease. Tagged MRI provides a promising new tool to help evaluate the effects of congenital anomalies and their treatment on cardiac function (Fogel et al., 1995, 1998).

Cardiac failure is an important and common health problem. Conventional assessments of failure have focused on global measures such as the ejection fraction. However, the additional measures of contractile function provided by tagged methods could potentially increase the ability to assess the degree of mechanical dysfunction in failure (MacGowan et al., 1997; Curry et al., 2000) and provide new criteria to detect its presence and monitor its progression and treatment. Approaches to augment LV function by surgical means can be evaluated with tagged MRI. These include both approaches employing the use of externally applied devices to reinforce the heart wall (Pilla et al., 2002) or augment ventricular filling or contraction (Pusca et al., 2000) and approaches to reshape the wall itself, so as to have a more advantageous size or shape (Kramer et al., 2002). If they were compatible with MRI, the effects on the ventricle of other implanted ventricular assist devices might be similarly studied with tagged MRI. Transplants can also be evaluated by tagged MRI (Donofrio et al., 1999). Stimulation by electrical pacing produces alterations in the mechanical activation of the myocardium that can be seen and measured with tagged MRI (Wyman et al., 1999). If acquired with sufficient temporal resolution, tagged MRI can show the progression of the wave of mechanical activation around the heart wall from the site of initial electrical activation at the pacing lead. This may lead to more insight into aspects of ventricular pacing such as its use in heart failure (Leclercq et al., 2002).

Stress–strain modeling of cardiac function is a promising potential application of the data derived from tagged MRI. In this case, we have the ability to directly

measure the dynamic changes in ventricular shape and regional strain over the cardiac cycle. However, we cannot directly determine the corresponding forces, or stress, within the wall from imaging; in fact, it is essentially impossible to reliably measure intramural stress even with invasive methods. Thus, if we can make "reasonable" estimates of the mechanical properties of the heart wall, based on our knowledge of the usual patterns of orientation of the muscle fibers within the wall and the mechanical properties of fresh tissue specimens as measured in vitro, we can model the expected distributions of the corresponding stress within the wall from the geometry and strains observed with MRI, together with additional boundary conditions from the pressures assumed within the ventricular cavity and outside the heart wall (Okamoto et al., 2000; Hu et al., 2003a,b).

5. Comparison with some alternative cardiac function imaging methods

While other imaging methods, including new multislice X-ray computed tomography, can provide good quality cross-sectional images of the moving heart, only MRI and ultrasound can provide noninvasive data on the motion patterns within the heart wall.

In addition to the ability to track material points through magnetization tagging, MRI offers the possibility of tracking their motion through motion-induced phase shifts in their MR signal. The origin of these shifts is the dependence of the frequency of the resonance on the local magnetic field strength; motion along magnetic field gradients like those used in MRI will generally result in a shift of the phase of the moving spins relative to that of adjacent stationary spins. Suitably designed MRI pulse sequences permit imaging of these motion-induced phase shifts. The need to acquire baseline data in order to correct for other sources of phase shift generally reduces the temporal resolution or increases the image acquisition time relative to comparable tagged imaging approaches. A given image will only provide one vector component of the motion; in general, three sets of such images will be needed to recover the full motion. As the phase shift will alias for values beyond $\pm 180°$, the motion sensitivity of the imaging must be adjusted to the range of the motion to be imaged. The MR signal can be acquired as a gradient echo, in which case the short duration of the measurement (limited by the T2 relaxation time) essentially results in a velocity measurement (Pelc et al., 1991). Alternatively, the MR signal can be acquired as a stimulated echo, in which case the longer duration of the measurement (limited by the longer T1 relaxation time) permits measurement of the net displacement over the measurement time, e.g., between end diastole and end systole (Aletras et al., 1999). The gradient echo phase shift imaging approach is readily adapted to multiphase "cine" imaging of velocity. Analysis of the wall motion from velocity maps will require integration over the cardiac cycle in order to calculate the net displacement as a function of time (Meyer et al., 1996). Integration error due to noise in the phase measurement can lead to corresponding errors in the displacement that can build up over the cardiac cycle and limit the reliability of the results. While the stimulated echo approach can directly yield displacement images, it is generally most readily adapted only to imaging of motion between fixed times in the cardiac cycle. Stimulated echoes also generally have poorer SNR (Kim et al., 2004).

Advantages of the phase shift techniques relative to tagging methods include simpler analysis, with no need to track the tags and interpolate the motion between them, potentially greater density of spatial sampling locations (although noisy data may require averaging of regional data with resulting loss of effective spatial resolution), and potentially greater sensitivity to small motions. Relative disadvantages of phase shift approaches include longer data acquisition times (or decreased temporal resolution), than tagging approaches and potential problems with phase aliasing. The use of tags also provides a more direct measure of displacement.

The principal approach used for ultrasound imaging of regional heart wall motion is the Doppler effect, the frequency shift of ultrasound reflected from a moving object. While more commonly employed for the study of the velocity of moving blood, it can also be used to image tissue velocity (Trambaiolo et al., 2001). In both cases, only the component of the velocity along the direction of the ultrasound beam can be measured. While the velocity is a point measurement, the variation of the velocity along the ultrasound beam can provide a measure of the rate of the deformation along this direction, the strain rate. Maps of these motion-related data can be created and displayed in essentially real time, e.g., as color overlays on the grayscale ultrasound image data. The principal weakness of this ultrasound method is the limitation of only being able to sample one component of the velocity vector or the strain rate tensor. The orientation of that component is limited by the available acoustic windows, a fundamental limitation of ultrasound imaging. In addition, if we wish to calculate the net displacement or strain, we must integrate over the cardiac cycle, leading to possible integration errors as with phase contrast MRI studies of tissue velocity. There may be additional errors due to the inability to account for motion in the unsampled directions.

6. Summary

While it still a relatively new area and is continuing to undergo active development, tagged MRI of cardiac

function promises to provide new insight into normal and abnormal cardiac function. Achieving a greater practical impact of tagged MRI will be dependent on the further development of more efficient methods of acquiring and analyzing the tagged image data. Challenges for tagged MRI include increasing spatial and temporal resolution while decreasing imaging time. While these are all competing objectives, ongoing advances in areas such as parallel imaging, respiratory motion compensation, and other aspects of data acquisition should enable further progress. Achieving good spatial registration between data acquired in different orientations is essential for 3D motion reconstruction, and will also benefit from improved imaging methods. Image processing and analysis will require development of methods with improved speed and reliability in order to permit more routine clinical applications of tagged MRI. Thus, further research in these areas could have important clinical rewards.

Acknowledgements

Dimitris Metaxas and a series of several students and programmers have contributed significantly to the development of tagged MRI methods in our laboratory. Grant support for this work was provided by the NIH through Grant RO1-HL-43014 and Grant RO1-LM-06638-01.

Appendix A. Supplementary data

Supplementary data associated with this article can be found, in the online version at doi:10.1016/j.media.2005.01.003.

References

Aletras, A.H., Ding, S., Balaban, R.S., Wen, H., 1999. DENSE: displacement encoding with stimulated echoes in cardiac functional MRI. Journal of Magnetic Resonance 137, 247–252.

Amini, A., Curwen, R., Constable, R., Gore, J., 1994. MR physics based snake tracking and dense deformations from tagged cardiac images. In: AAAI International Symposium on Computer Vision and Medical Image Processing.

Amini, A., Chen, Y., Curwen, R., Mani, V., Sun, J., 1998. Coupled B-snake grids and constrained thin-plate splines for analysis of 2D tissue deformations from tagged MRI. IEEE Transactions on Medical Imaging 17 (3), 344–356.

Amini, A., Prince, J., 2001. Measurement of Cardiac Deformations from MRI: Physical and Mathematical Models. Kluwer Academic Publishers, Dordrecht.

Augenstein, K., Young, A., 2001. Ch 3: Finite element modeling for three-dimensional motion reconstruction and analysis. In: Amini, A., Prince, J. (Eds.), Measurement of Cardiac Deformations from MRI: Physical and Mathematical Models. Kluwer Academic Publishers, Dordrecht.

Axel, L., Costantini, J., Listerud, J., 1987. Intensity correction in surface-coil MR imaging. American Journal of Radiology 148, 418–420.

Axel, L., Dougherty, L., 1989a. MR imaging of motion with spatial modulation of magnetization. Radiology 171, 841–845.

Axel, L., Dougherty, L., 1989b. Heart wall motion: improved method of spatial modulation of magnetization for MR imaging. Radiology 172, 349–350.

Axel, L., Goncalves, R.C., Bloomgarden, D., 1992. Regional heart wall motion: two-dimensional analysis and functional imaging with MR imaging. Radiology 183 (3), 745–750.

Behloul, F., Lelieveldt, B.P., Boudraa, A., Janier, M.F., Revel, D., Reiber, J.H., 2001. Neuro-fuzzy systems for computer-aided myocardial viability assessment. IEEE Transactions on Medical Imaging 20 (12), 1302–1313.

Bergey, P.D., Axel, L., 2000. Focal hypertrophic cardiomyopathy simulating a mass: MR tagging for correct diagnosis. American Journal of Radiology 174, 242–244.

Bogaert, J., Maes, A., Van de Werf, F., Bosmans, H., Herregods, M.-C., Nuyts, J., Desmet, W., Mortelmans, L., Marchal, G., Rademakers, F.E., 1999. Functional recovery of subepicardial myocardial tissue in transmural myocardial infarction after successful reperfusion. Circulation 99, 36–43.

Bogaert, J., Rademakers, F., 2001. Regional nonuniformity of normal adult human left ventricle. American Journal of Physiology-Heart and Circulatory Physiology 280, H610–H620.

Bolster Jr., B.D., McVeigh, E.R., Zerhouni, E.A., 1990. Myocardial tagging in polar coordinates with use of striped tags. Radiology 177, 769–772.

Bouton, S., Yang, A., McCrindle, B.W., Kidd, L., McVeigh, E.R., Zerhouni, E.A., 1991. Differentiation of tumor from viable myocardium using cardiac tagging with MR imaging. Journal of Computer Assisted Tomography 15, 676–678.

Chandrashekara, R., Mohiaddin, R.H., Rueckert, D., 2002. Analysis of myocardial motion in tagged MR images using non-rigid image registration. In: Proceedings of the SPIE Medica Imaging 2002: Image Processing, pp. 1168–1179.

Chen, Y., Amini, A., 2001. A MAP framework for tag line detection in SPAMM data using Markov random fields on the B-spline solid. In: IEEE Workshop on Mathematical Methods in Biomedical Image Analysis, pp. 131–138.

Clarysse, P., Basset, C., Khouas, L., Croisille, P., Friboulet, D., Odet, C., Magnin, I.E., 2000. 2D spatial and temporal displacement field fitting from cardiac MR tagging. Medical Image Analysis 4, 253–268.

Croisille, P., Moore, C.C., Judd, R.M., Lima, J.A.C., Arai, M., McVeigh, E.R., Becker, L.C., Zerhouni, E.A., 1999. Differentiation of viable and nonviable myocardium by the use of three-dimensional tagged MRI in 2-day-old reperfused canine infarcts. Circulation 99, 284–291.

Curry, C.W., Nelson, G.S., Wyman, B.T., Declerck, J., Talbot, M., Berger, R.D., McVeigh, E.R., Kass, D.A., 2000. Mechanical dyssynchrony in dilated cardiomyopathy with intraventricular conduction delay as depicted by3D tagged magnetic resonance imaging. Circulation 101, 2e.

Declerck, J., Feldmar, J., Ayache, N., 1998. Definition of a 4D continuous planispheric transformation for the tracking and the analysis of LV motion. Medical Image Analysis 2 (2), 197–213.

Deng, X., Denney, T., 2003. Rapid 3D LV strain reconstruction from tagged cardiac MR images. Proceedings of ISMRM 11, #707.

Denney, T., 1997. Identification of myocardial tags in tagged MR images without prior knowledge of myocardial contours. In: Duncan, James S., Gindi, Gene (Eds.), Information Processing in Medical Imaging, 15th International Conference, IPMI'97, Poultney, Vermont, USA, June 9–13, 1997, Proceedings, Lecture Notes in Computer Science, vol. 1230. Springer, Berklin, pp. 327–340, ISBN 3-540-63046-5.

Denney, T., Prince, J., 1994. Optimal brightness functions for optical flow estimation of deformable motion. IEEE Transactions on Image Processing 3 (2), 178–191.

Dong, S.-J., Crawley, A.P., MacGregor, J.H., Petrank, Y.F., Bergman, D.W., Belenkie, I., Smith, E.R., Tyberg, J.V., Beyar, R., 1995. Regional left ventricular systolic function in relation to the cavity geometry in patients with chronic right ventricular pressure overload: a three-dimensional tagged magnetic resonance imaging study. Circulation 91, 2359–2370.

Dong, S.-J., Hees, P.S., Huang, W.-M., Buffer, S.A., Weiss, J.L., Shapiro, E.P., 1999. Independent effects of preload, afterload, and contractility on left ventricular torsion. American Journal of Physiology-Heart and Circulatory Physiology 277, H1053–H1060.

Dong, S.-J., Hees, P.S., Siu, C.O., Weiss, J.L., Shapiro, E.P., 2001. MRI assessment of LV relaxation by untwisting rate: a new isovolumetric phase measure of t. American Journal of Physiology-Heart and Circulatory Physiology 281, H2002–H2009.

Donofrio, M.T., Clark, B.J., Ramaciotti, C., Jacobs, M.L., Fellows, K.E., Weinberg, P.M., Fogel, M.A., 1999. Regional wall motion and strain of transplanted hearts in pediatric patients using magnetic resonance tagging. American Journal of Physiology 277 (5 Pt 2), R1481–R1487.

Dornier, C., Ivancevic, M., Lecoq, G., Osman, N., Foxall, D., Righetti, A., Vallée, J., 2002. Assessment of the left ventricle ejection fraction by MRI tagging: comparisons with cine MRI and coronary angiography. In: Proceedings of ISMRM, vol. 10, #1680.

Dougherty, L., Asmuth, J., Blom, A., Axel, L., Kumar, R., 1999. Validation of an optical flow method for tag displacement estimation. IEEE Transactions on Medical Imaging 18 (4), 359–363.

Edelman, R.R., Manning, W.J., Burstein, D., Paulin, S., 1991. Coronary arteries: breath-hold MR angiography [see comments]. Radiology 181, 641–643.

Ehman, R.L., Felmlee, J.P., 1989. Adaptive technique for high-definition MR imaging of moving structures. Radiology 173, 255–263.

Ehman, R.L., McNamara, M.T., Pallack, M., Hricak, H., Higgins, C.B., 1984. Magnetic resonance imaging with respiratory gating: techniques and advantages. American Journal of Roentgenology 143, 1175–1182.

Epstein, F.H., Wolff, S.D., Arai, A.E., 1999. Segmented k-space fast cardiac imaging using an echo-train readout. Magnetic Resonance in Medicine 41, 609–613.

Fayad, Z.A., Ferrari, V.A., Kraitchman, D.L., Young, A.A., Palevsky, H.I., Bloomgarden, D.C., Axel, L., 1998. Right ventricular regional function using MR tagging: normals versus chronic pulmonary hypertension. Magnetic Resonance in Medicine 39 (1), 116–123.

Fischer, S.E., McKinnon, G.C., Maier, S.E., Boesiger, P., 1993. Improved myocardial tagging contrast. Magnetic Resonance in Medicine 30, 191–200.

Fischer, S.E., McKinnon, G.C., Scheidegger, M.B., Prins, W., Meier, D., Boesiger, P., 1994. True myocardial motion tracking. Magnetic Resonance in Medicine 31, 401–413.

Fogel, M.A., Weinberg, P.M., Fellows, K.E., Hoffman, E.A., 1995. A study in ventricular–ventricular interaction. Circulation 92, 219–230.

Fogel, M.A., Weinberg, P.M., Gupta, K.B., Rychik, J., Hubbard, A., Hoffman, E.A., Haselgrove, J., 1998. Mechanics of the single ventricle. A study in ventricular–ventricular intersction II. Circulation 98, 330–338.

Fogel, M.A., Weinberg, P.M., Hubbard, A., Haselgrove, J., 2000. Diastolic biomechanics in normal infants utilizing MRI tissue tagging. Circulation 102, 218–224.

Fonseca, C.G., Oxenham, H.C., Cowan, B.R., Occleshaw, C.J., Young, A.A., 2003. Aging alters patterns of regional nonuniformity in LV strain relaxation: a 3-D MR tissue tagging study. American Journal of Physiology-Heart and Circulatory Physiology 285, H621–H630.

Garot, J., Bluemke, D., Osman, N., Rochitte, C., McVeigh, E., Zerhouni, E., Prince, J., Lima, J., 2000. Fast determination of regional myocardial strain fields from tagged cardiac images using harmonic phase (HARP) magnetic resonance imaging. Circulation 101, 981–988.

Geskin, G., Kramer, C.M., Rogers, W.R., Theobald, T.M., Pasktis, D., Hu, Y-L., Reichek, N., 1998. Quantitative assessment of myocardial viability after infarction by dobutamine magnetic resonance tagging. Circulation 98, 217–223.

Goette, M.J., van Rossum, A.C., Twisk, J.W.R., Kuijer, J.P.A., Marcus, J.T., Visser, C.A., 2001. Quantification of regional contractile function after infarction: strain analysis superior to wall thickening analysis in discriminating infarct from remote myocardium [comment]. Journal of the American College of Cardiology 37, 808–817.

Goutsias, J., Batman, S., 2000. Ch 4: Morphological methods for biomedical image analysis. In: Sonka, M., Fitzpatrick, J (Eds.), Handbook of Medical Imaging: Medical Imaging Processing and Analysis, vol. 2. SPIE, pp. 255–263.

Guttman, M., Prince, J., McVeigh, E., 1994. Tag and contour detection in tagged MR images of the left ventricle. IEEE Transactions on Medical Imaging 13 (1), 74–88.

Guttman, M., Zerhouni, E., McVeigh, E., 1997. Analysis and visualization of cardiac function from MR images. IEEE Computer Graphics and Applications 17 (1), 30–38.

Haber, I., 2000a. Three-dimensional motion reconstruction and analysis of the right ventricle from planar tagged MRI. Ph.D. Thesis, Univ. of Penn.

Haber, I., Metaxas, D.N., Axel, L., 2000b. Three-dimensional motion reconstruction and analysis of the right ventricle using tagged MRI. Medical Image Analysis 4, 335–355.

Haber, I., Kikinis, R., Westin, C., 2001. Phase-driven finite element model for spatio-temporal tracking in tagged cardiac MRI. In: Niessen, W.J., Viergever, M.A. (Eds.), Proceedings of Medical Image Computing and Computer-assisted Intervention, Utrecht, Netherlands, LCNS, vol. 2208. Springer, Berlin, pp. 1332–1335.

Herzka, D.A., Guttman, M.A., McVeigh, E.R., 2003. Myocardial tagging with SSFP. Magnetic Resonance in Medicine 49, 329–340.

Hu, Z., Metaxis, D., Axel, L., 2003a. In vivo strain and stress estimation of the heart left and right ventricles from MRI images. Medical Image Analysis 7, 435–444.

Hu, Z., Metaxas, D., Axel, L., 2003b. Left ventricle composite material model for strain–stress analysis. In: 2003 International Symposium on Surgery Simulation and Soft Tissue Modeling, Juan-Les-Pins, FranceLCNS, vol. 2673. Springer, Berlin, pp. 218–229.

Huang, J., Abendschein, D., Davila-Roman, V., Amini, A., 1999. Spatio-temporal tracking of myocardial deformations with a 4D B-spline model from tagged MRI. IEEE Transactions on Medical Imaging 18 (10), 957–972.

Kerwin, W., Prince, J., 1998. Cardiac material markers from tagged MR images. Medical Image Analysis 2 (4), 339–353.

Kim, D., Bove, C.M., Kramer, C.M., Epstein, F.H., 2003. Importance of *k*-space trajectory in echo-planar myocardial tagging at rest and during dobutamine stress. Magnetic Resonance in Medicine 50, 813–820.

Kim, D., Epstein, F.H., Gilson, W.D., Axel, L., 2004. Increasing the signal-to-noise ratio in DENSE MRI by combining displacement-encoded echoes. Magnetic Resonance in Medicine 52, 188–192.

Kojima, S., Yamada, N., Goto, Y., 1999. Diagnosis of constrictive pericarditis by tagged cine magnetic resonance imaging. NEJM 341, 373–374.

Korin, H.W., Felmlee, J.P., Ehman, R.L., Riederer, S.J., 1990. Adaptive technique for three-dimensional MR imaging of moving structures. Radiology 177, 217–221.

Kraitchman, D., Young, A., Chang, C., Axel, L., 1995. Semi-automated tracking of myocardial motion in MR tagged images. IEEE Transactions on Medical Imaging 14, 422–433.

Kraitchman, D.L., Sampath, S., Castillo, E., Derbyshire, J.A., Boston, R.C., Bluemke, D.A., Gerber, B.L., Prince, J.L., Osman, N.F., 2003. Quantitative ischemia detection during cardiac magnetic resonance stress testing by use of fastHARP. Circulation 107, 2025–2030.

Kramer, C.M., Reichek, N., Ferrari, V.A., Dawson, J., Axel, L., 1994. Regional heterogeneity of function in hypertrophic cardiomyopathy. Circulation 90, 184–194.

Kramer, C.M., Ferrari, V.A., Rogers, W.J., Theobald, T.M., Nance, M.L., Axel, L., Reichek, N., 1996a. Angiotensin-converting enzyme inhibition limits dysfunction in adjacent noninfarcted regions during left ventricular remodeling. Journal of the American College of Cardiology 27 (1), 211–217.

Kramer C.M, Rogers, W.J., Theobald, T.M., Power, T.P., Petrulo, S., Reichek, N., 1996b. Remote noninfarcted region dysfunction soon after first anterior myocardial infarction. Circulation 94, 660–666.

Kramer, C.M., Magovern, J.A., Rogers, W.J., Vido, D., Savage, E.B., 2002. Reverse remodeling and improved regional function after repair of left ventricular aneurysm. Journal of Thoracic and Cardiovascular Surgery 123, 700–706.

Kuijpers, D., Ho, K.Y., van Dijkman, P.R., Vliegenthart, R., Oudkerk, M., 2003. Dobutamine cardiovascular magnetic resonance for the detection of myocardial ischemia with the use of myocardial tagging. Circulation 107, 1592–1597.

Kumar, S., Goldgof, D., 1994. Automatic tracking of SPAMM grid and the estimation of deformation parameters from cardiac images. IEEE Transactions on Medical Imaging 13 (1), 122–132.

Leclercq, C., Faris, O., Tunin, R., Johnson, J., Kato, R., Evans, F., Spinelli, J., Halperin, H., McVeigh, E., Kass, D.A., 2002. Systolic improvement and mechanical resynchronization does not require electrical synchrony in the dilated failing heart with left bundle-branch block. Circulation 106 (14), 1760–1763.

Lima, J.A., Jeremy, R., Guier, W., Bouton, S., Zerhouni, E.A., McVeigh, E., Buchalter, M.B., Weisfeldt, M.L., Shapiro, E.P., Weiss, J.L., 1993. Accurate systolic wall thickening by nuclear magnetic resonance imaging with tissue tagging: correlation with sonomicrometers in normal and ischemic myocardium. Journal of the American College of Cardiology 21, 1741–1751.

Lorenz, C.H., Pastorek, J.S., Bundy, J.M., 2000. Delineation of normal human left ventricular twist throughout systole by tagged cine magnetic resonance imaging. Journal of Cardiovascular Magnetic Resonance 2 (2), 97–108.

MacGowan, G.A., Shapiro, E.P., Azhari, H., Siu, C.O., Hees, P., Hutchins, G.M., Weiss, J.L., Rademakers, F.E., 1997. Noninvasive measurement of shortening in the fiber and cross-fiber directions in the normal left ventricle and in idiopathic dilated cardiomyopathy. Circulation 96, 535–541.

Marcus, J.T., Götte, M.J.W., Van Rossum, A.C., Kuijer, J.P.A., Heethaar, R.M., Axel, L., Visser, C.A., 1997. Myocardial function in infarcted and remote regions early after infarction in man: assessment by magnetic resonance tagging and strain analysis. Magnetic Resonance in Medicine 38, 803–810.

McQueen, D., Peskin, C., 2000. Heart simulation by an immersed boundary method with formal second-order accuracy and reduced numerical viscosity. In: Aref, H., Phillips, J.W. (Eds.), Mechanics for a New Millennium. Proceedings of the International Conference on Theoretical and Applied Mechanics (ICTAM) 2000. Kluwer Academic Publishers, Dordrecht, pp. 429–444.

McVeigh, E.R., Atalar, E., 1992. Cardiac tagging with breath-hold cine MRI. Magnetic Resonance in Medicine 28, 318–327.

Meyer, F.G., Constable, R.T., SInusas, A.J., Duncan, J.S., 1996. Tracking myocardial deformation using phase contrast MR velocity fields: a stochastic approach. IEEE Transactions on Medical Imaging 15, 453–465.

Montillo, A., Metaxas, D., Axel, L., 2002. Automated segmentation of the left and right ventricles in 4D cardiac SPAMM images. In: Dohi, T., Kikinis, R. (Eds.), Proceedings of Medical Image Computing and Computer-assisted Intervention, Tokyo, Japan, LCNS, vol. 2488. Springer, Berlin, pp. 620–633.

Montillo, A., Axel, L., Metaxas, D., 2003a. Automated correction of background intensity variation and image scale standardization in 4D cardiac SPAMM-MRI. In: Proceedings of International Society for Magnetic Resonance in Medicine, Toronto, Canada, #708.

Montillo, A., Udupa, J., Axel, L., Metaxas, D., 2003b. Interaction between noise suppression and inhomogeneity correction in MRI. In: Proceedings of SPIE: Medical Imaging, San Diego, CA, vol. 5032, pp. 1025–1036.

Montillo, A., Metaxas, D., Axel, L., 2003c. Automated deformable model-based segmentation of the left and right ventricles in tagged cardiac MRI. In: Ellis, R.E., Peters, T.M. (Eds.), Proceedings of Medical Image Computing and Computer-assisted Intervention, Montreal, Canada, LCNS, vol. 2878. Springer, Berlin, pp. 507–515.

Moore, C.C., Reeder, S.B., McVeigh, E.R., 1994. Tagged MR imaging in a deforming phantom: photographic validation. Radiology 190, 765–769.

Moore, C.C., Logo-Olivieri, C.H., McVeigh, E.R., Zerhouni, E.A., 2000. Three-dimensional systolic strain paterns in the normal human left ventricle: characterization with tagged MR imaging. Radiology 214, 453–466.

Morse, O.C., Singer, J.R., 1970. Blood velocity measurements in intact subjects. Science 170, 440–441.

Moses, D., Axel, L., 2004. Quantification of curvature and shape of the interventricular septum. Magnetic Resonance in Medicine 52, 154–163.

Mosher, T.J., Smith, M.B., 1990. A DANTE tagging sequence for the evaluation of translational sample motion. Magnetic Resonance in Medicine 15, 334–339.

Nyul, L., Udupa, J., Zhang, X., 2000. New variants of a method of MRI scale standardization. IEEE Transactions on Medical Imaging 19 (2), 143–150.

O'Dell, W., Moore, C., Hunter, W., Zerhouni, E., McVeigh, E., 1995. Displacement field fitting for calculating 3D myocardium deformation from tagged images. Radiology 195, 829–835.

O'Dell, W.G., McCulloch, A.D., 2000. Imaging three-dimensional cardiac function. Annual Review Biomedical Engineering 2, 431–456.

Okamoto, R.J., Moulton, M.J., Peterson, S.J., Li, D., Pasque, M.K., Guccione, J.M., 2000. Epicardial suction: a new approach to mechanical testing of the passive ventricular wall. Journal of Biomechanical Engineering 122 (5), 479–487.

Osman, N.F., Kerwin, W.S., McVeigh, E.R., Prince, J.L., 1999. Cardiac motion tracking using CINE harmonic phase (HARP) magnetic resonance imaging. Magnetic Resonance in Medicine 42, 1048–1060.

Osman, N., Garot, J., Sampath, S., Gerber, B., Wu, K., Atalar, E., Lima, J., Prince, J., 2002. Imaging longitudinal cardiac strain on short-axis images using strain-encoded MRI. Magnetic Resonance in Medicine 46, 324–334.

Ozturk, C., McVeigh, E., 1999. Four dimensional B-spline based motion analysis of tagged cardiac MR images. In: Proceedings of SPIE Medical Imaging 99, San Diego, CA, pp. 46–56.

Palmon, L.C., Reichek, N., Yeon, S.B., Clark, N.R., Brownson, D., Hoffman, E., Axel, L., 1994. Intramural myocardial shortening in hypertensive left ventricular hypertrophy with normal pump function. Circulation 89, 122–131.

Park, J., Metaxas, D., Young, A., Axel, L., 1996. Deformable models with parameter functions for cardiac motion analysis. IEEE Transactions on Medical Imaging 15 (3), 278–289.

Park, K., Metaxas, D., Axel, L., 2003. A finite element model for functional analysis of 4D cardiac-tagged MR images. In: Ellis,

R.E., Peters, T.M. (Eds.), Proceedings of Medical Image Computing and Computer-assisted Intervention, Montreal, Canada, LCNS, vol. 2878. Springer, Berlin, pp. 491–498.

Pelc, N.J., Herfkens, R.J., Shimakawa, A., Enzmann, D.R., 1991. Phase contrast cine magnetic resonance imaging. Magnetic Resonance Quarterly 7, 229–254.

Peters, D.C., Epstein, F.H., McVeigh, E.R., 2001. Myocardial wall tagging with undersampled projection reconstruction. Magnetic Resonance in Medicine 45, 562–567.

Pilla, J.J., Blom, A.S., Brockman, D.J., Bowen, F., Yuan, Q., Giammarco, J., Ferrari, V.A., Gorman III, J.H., Gorman, R.C., Acker, M.A., 2002. Ventricular constraint using the Acorn cardiac support device reduces myocardial akinetic area in an ovine model of acute infarction. Circulation 106 (Suppl. I), I-207–I-211.

Prince, J., McVeigh, E., 1992. Motion estimation from tagged MR image sequences. IEEE Transactions on Medical Imaging 11 (2), 238–249.

Pusca, S.V., Pilla, J.J., Blom, A.S., Patel, H.J., Yuan, Q., Ferrari, V.A., Prood, C., Axel, L., Acker, M.A., 2000. Assessment of synchronized direct mechanical ventricular actuation in a canine model of left ventricular dysfunction. ASAIO Journal 46, 756–760.

Qian, Z., Montillo, A., Metaxas, D., Axel, L., 2003. Segmenting cardiac MRI tagging lines using Gabor filter banks. In: Proceedings of International Conference of the Engineering in Medicine and Biology Society, Cancun, Mexico, pp. 630–633.

Radeva, P., Amini, A., Huang, J., 1997. Deformable B-Solids and implicit snakes for 3D localization and tracking of SPAMM MRI data. Computer Vision and Image Understanding 66, 163–178.

Reeder, S.B., McVeigh, E.R., 1994. Tag contrast in breath-hold CINE cardiac MRI. Magnetic Resonance in Medicine 31, 521–525.

Reeder, S.B., Atalar, E., Faranesh, A.Z., McVeigh, E.R., 1999. Multi-echo segmented k-space imaging: an optimized hybrid sequence for ultrafast cardiac imaging. Magnetic Resonance in Medicine 41, 375–385.

Rogers Jr., W.J., Shapiro, E.P., Weiss, J.L., Buchalter, M.B., Rademakers, F.E., Weisfeldt, M.L., Zerhouni, E.A., 1991. Quantification of and correction for left ventricular systolic long-axis shortening by magnetic resonance tissue tagging and slice isolation. Circulation 84, 721–731.

Ryf, S., Spiegel, M.A., Gerber, M., Boesiger, P., 2002. Myocardial tagging with 3D-CSPAMM. Journal of Magnetic Resonance Imaging 16, 320–325.

Ryf, S., Kissinger, K.V., Spiegel, M.A., Bornert, P., Manning, W.J., Boesiger, P., Stuber, M., 2004. Spiral MR myocardial tagging. Magnetic Resonance in Medicine 2004 51, 237–242.

Sachs, T.S., Meyer, C.H., Irarrazabal, P., Hu, B.S., Nishimura, D.G., Macovski, A., 1995. The diminishing variance algorithm for real-time reduction of motion artifacts in MRI. Magnetic Resonance in Medicine 34, 412–422.

Saha, P., Udupa, J., 2001. Scale-based image filtering preserving boundary sharpness and fine structure. IEEE Transactions on Medical Imaging 20, 1140–1155.

Sandstede, J.J.W., Johnson, T., Haare, K., Beer, M., Hofmann, S., Pabst, T., Kenn, W., Voelker, W., Neubauer, S., Hahn, D., 2002. Cardiac systolic rotation and contraction before and after valve replacement of aortic stenosis: a myocardial tagging study using MR imaging. American Journal of Roentgenology. 178, 953–958.

Scott, C.H., St. John Sutton, M.G., Gusani, N., Fayad, Z., Kraitchman, D., Keane, M.G., Axel, L., Ferrari, V.A., 1999. Effect of dobutamine on regional left ventricular function measured by tagged magnetic resonance imaging in normal subjects. American Journal of Cardiology 83, 412–417.

Sermesant, M., Coudire, Y., Delingette, H., Ayache, N., 2002. Progress towards an electromechanical model of the heart for cardiac image analysis. In: IEEE International Symposium on Biomedical Imaging (ISBI'02), pp. 10–14.

Sled, J., Zijdenbos, A., Evans, A., 1998. A nonparametric method for automatic correction of intensity nonuniformity in MRI data. IEEE Transactions on Medical Imaging 17 (1), 87–97.

Stuber, M., Fischer, S.E., Scheidegger, M.B., Boesiger, P., 1999a. Toward high-resolution myocardial tagging. Magnetic Resonance in Medicine 41, 639–643.

Stuber, M., Spiegel, M., Fischer, S., Scheidegger, M., Danias, P., Pedersen, E., Boesiger, P., 1999b. Single breath-hold slice-following CSPAMM myocardial tagging. MAGMA Magnetic Resonance Materials in Physics, Biology and Medecine 9, 85–91.

Stuber, M., Scheidegger, M.B., Fischer, S.E., Nagel, E., Steinmann, F., Hess, O.M., Boesiger, P., 1999c. Alterations in the local myocardial motion pattern in patients suffering form pressure overload due to aortic stenosis. Circulation 100, 361–368.

Tang, C., McVeigh, E.R., Zerhouni, E.A., 1995. Multi-shot EPI for improvement of myocardial tag contrast: comparison with segmented SPGR. Magnetic Resonance in Medicine 33, 443–447.

Trambaiolo, P., Tonti, G., Salustri, A., Fedele, F., Sutherland, G., 2001. New insights into regional systolic and diastolic left ventricular function with tissue Doppler echocardiography: from qualitative analysis to a quantitative approach. Journal of American Society of Echocardiography 14, 85–96.

Van Dijk, P., 1984. Direct cardiac NMR imaging of heart wall and blood flow velocity. Journal of Computer Assisted Tomography 8 (3), 429–436.

Wells, W., Grimson, W., Kikinis, R., Jolesz, F., 1996. Adaptive segmentation of MRI data. IEEE Transactions on Medical Imaging 15, 429–442.

Wu, E.X., Towe, C.W., Tang, H., 2002. MRI cardiac tagging using a sinc-modulated RF pulse train. Magnetic Resonance in Medicine 48, 389–393.

Wyman, B.T., Hunter, W.C., Prinzen, E.W., McVeigh, E.R., 1999. Mapping propagation of mechanical activation in the paced heart with MRI tagging. American Journal of Physiology-Heart and Circulatory Physiology 276 (45), H881–H891.

Yeon, S.B., Reichek, N., Tallant, B.A., Lima, J.A., Calhoun, L.P., Clark, N.R., Hoffman, E.A., Ho, K.K., Axel, L., 2001. Validation of in vivo myocardial strain measurement by magnetic resonance tagging with sonomicrometry. Journal of the American College of Cardiology 38, 555–561.

Young, A.A., Axel, L., 1992. Three-dimensional motion and deformation of the heart wall: estimation with spatial modulation of magnetization – a model-based approach. Radiology 185 (1), 241–247.

Young, A.A., Axel, L., Dougherty, L., Bogen, D.K., Parenteau, C.S., 1993. Validation of tagging with MR imaging to estimate material deformation. Radiology 188, 101–108.

Young, A.A., Imai, H., Chang, C.N., Axel, L., 1994a. Two-dimensional left ventricular deformation during systole using magnetic resonance imaging with spatial modulation of magnetization. Circulation 89 (2), 740–752.

Young, A., Kramer, C.M., Ferrari, V.A., Axel, L., Reichek, N., 1994b. Three-dimensional left ventricular deformation in hypertrophic cardiomyopathy. Circulation 90, 854–867.

Young, A., Kraitchman, D., Dougherty, L., Axel, L., 1995. Tracking and finite element analysis of stripe deformation in magnetic resonance tagging. IEEE Transactions on Medical Imaging 14, 413–421.

Young, A.A., Fayad, Z.A., Axel, L., 1996. Right ventricular midwall surface motion and deformation using magnetic resonance tagging. American Journal of Physiology-Heart and Circulatory Physiology 271 (6 Pt. 2), H2677–H2688.

Young, A., 1998. Model tags: direct 3D tracking of heart wall motion from tagged magnetic resonance images. In: Wells, W.M., Col-

chester, Delp, S. (Eds.), Proceedings of Medical Image Computing and Computer-assisted Intervention, Boston, October 11–13, 1998, Lecture Notes in Computer Science, vol. 1496. Springer, Cambridge, pp. 92–101.

Young, A., 1999. Model tags: direct 3D tracking of heart wall motion from tagged magnetic resonance images. Medical Image Analysis 3, 361–372.

Yuan, Q., Axel, L., Hernandez, E.H., Dougherty, L., Pilla, J.J., Scott, C.H., Ferrari, V.A., Blom, A.S., 2000. Cardiac-respiratory gating method for magnetic resonance imaging of the heart. Magnetic Resonance in Medicine 43, 314–318.

Zerhouni, E.A., Parish, D.M., Rogers, W.J., Yang, A., Shapiro, E.P., 1988. Human heart: tagging with MR imaging – a method for noninvasive assessment of myocardial motion. Radiology 169, 59–63.

Zwanenburg, J.J., Kuijer, J.P., Marcus, J.T., Heethaar, R.M., 2003. Steady-state free precession with myocardial tagging: CSPAMM in a single breathhold. Magnetic Resonance in Medicine 49, 722–730.